# Modelling of the fragmentation process in brittle solids based on x-ray micro-tomography analysis

## P. FORQUIN[a], M. BLASONE[a], D. GEORGES[b], M. DARGAUD[a], E. ANDO[a]

a. Univ. Grenoble Alpes, CNRS, Grenoble INP, 3SR, F-38000 Grenoble, France,
{pascal.forquin, maria.blasone, marielle.dargaud, edward.ando}@3sr-grenoble.fr
b. Univ. Grenoble Alpes, CNRS, Grenoble INP, 3SR/IGE, F-38000 Grenoble, France,
david.georges@univ-grenoble-alpes.fr

## Résumé :

*Les géomatériaux et autres matériaux fragiles tels que les bétons, les roches, le verre, la glace de grêlons, les céramiques sont présents dans de nombreuses problématiques de recherche industrielles ou du génie civil faisant intervenir des conditions de chargement de traction dynamique. Sous de telles conditions de chargement les matériaux fragiles subissent un processus de fragmentation multiple constitué de nombreuses fissures orientées déclenchées sur des défauts critiques. Cependant, faute de données sur les défauts activés à très petite échelle, le processus de fragmentation reste difficile à modéliser. La chaire Brittle's CODEX vise à mieux comprendre le lien entre les paramètres microstructuraux des matériaux fragiles et leur réponse sous chargement à très haute vitesse de déformation. Dans la présente contribution, un modèle analytique du processus de fragmentation dynamique est développé en considérant une distribution quelconque de défauts critiques. Dans un deuxième temps, les microstructures de trois matériaux fragiles sont analysées par tomographie à rayons X. Sur la base de ces données expérimentales les propriétés de fragmentation dynamique d'une de ces microstructures sont prédites en fonction de la vitesse de chargement.*

## Abstract:

*Brittle materials are subjected to high-strain-rates tensile loadings in various conditions such as in protective structures subjected to impact or blast, in the mining industry or in various industrial processes. Under very high strain-rate loadings, brittle materials experience a multiple-fragmentation process made of numerous oriented cracks triggered on critical defects. However due to a lack of data regarding the activated defects at very small scale the fragmentation process remains difficult to model. The Brittle's CODEX chair aims to gain insight into the link between the microstructural parameters of brittle materials and their response under very high-strain-rate loading. In the present contribution, a closed form solution of the fragmentation process is developed considering any populations of critical defects. Secondly, the microstructure of three brittle materials is being analysed by using x-ray micro-tomography. Based on these experimental data the dynamic fragmentation properties of one of these materials are predicted as function of the applied loading rate.*

**Keywords: Brittle materials, Microstructure, Fragmentation, Modelling, X-ray Tomography**

# 1      Introduction

Brittle materials are extensively employed in many civil and military applications involving high-strain-rate loadings such as: blasting or percussive drilling of rocks, ballistic impact against ceramic armour or transparent windshields, plastic explosives employed to damage or destroy concrete structures, soft or hard impacts against concrete structures, etc. In all of these applications, brittle materials are subjected to intense loadings characterized by medium to extremely high strain-rates (few tens to several tens of thousands $s^{-1}$) leading to extreme and/or specific damage modes such as multiple fragmentation, dynamic cracking, pore collapse, spalling, mode II fracturing, etc... Additionally, brittle materials exhibit complex features such as strong strain-rate sensitivity and a transition from a probabilistic response at low strain-rates to a deterministic behaviour at high-strain-rates that justify expending greater research efforts to understand these complex features.

The aim of the present work is to illustrate how the distribution of critical defects may influence the dynamic fragmentation properties at high strain-rates. In the first part of the paper the basis of the fragmentation model are detailed. In the second part predictions of the model

# 2      Modelling of multiple fragmentation process in brittle solids: the DFH (Denoual-Forquin-Hild) model

The fragmentation process induced in brittle materials under high-strain-rates tensile loadings corresponds to the initiation and propagation of a large number of cracks from volume or surface defects that exist in a structure $\Omega$ of size Z, Z being a length, a surface area, or a volume. The point defects can be assumed to be randomly distributed and activated at various or random level of stress that can be a function of the size of each defect as considered in (Jayatilaka and Trustrum, 1977). The number of critical defects in Z (i.e., whose activation stress is exceeded) can be described by a density of critical defects related to the applied stress level $\lambda_t(\sigma)$. The schematic of a fragmentation process is illustrated in the Figure 1. Defects are distributed along the horizontal axis that represents the spatial scale and the vertical axis that represents the time-scale or stress-level scale assuming that the stress level varies linearly or monotonously with time. As the stress level is increasing ($\overset{\circ}{\sigma} > 0$), the number of critical defects increases. However, the first cracks that propagate from the first critical defects relax stresses in their vicinity ($\overset{\circ}{\sigma} < 0$) and prevent the activation of critical defects in an "obscured domain" of size $Z_o(T - t)$ centred on this crack, where $T - t$ corresponds to the time interval between the crack inception $t$ and the current time $T$. The growth of obscuration domains (i.e., zones in which $\overset{\circ}{\sigma} < 0$) from activated defects is depicted by triangles (obscuration hyper-cones) in the Figure 1, assuming a constant propagation velocity. The fragmentation process ends when the whole domain is obscured.

The fragmentation process can be described through the obscuration probability concept by considering the condition (in terms of probability) for a point $M$ at a time $T$ not to be obscured, i.e., able to initiate a new crack from a critical defect that would exit at that point $M$ activated at time $T$.
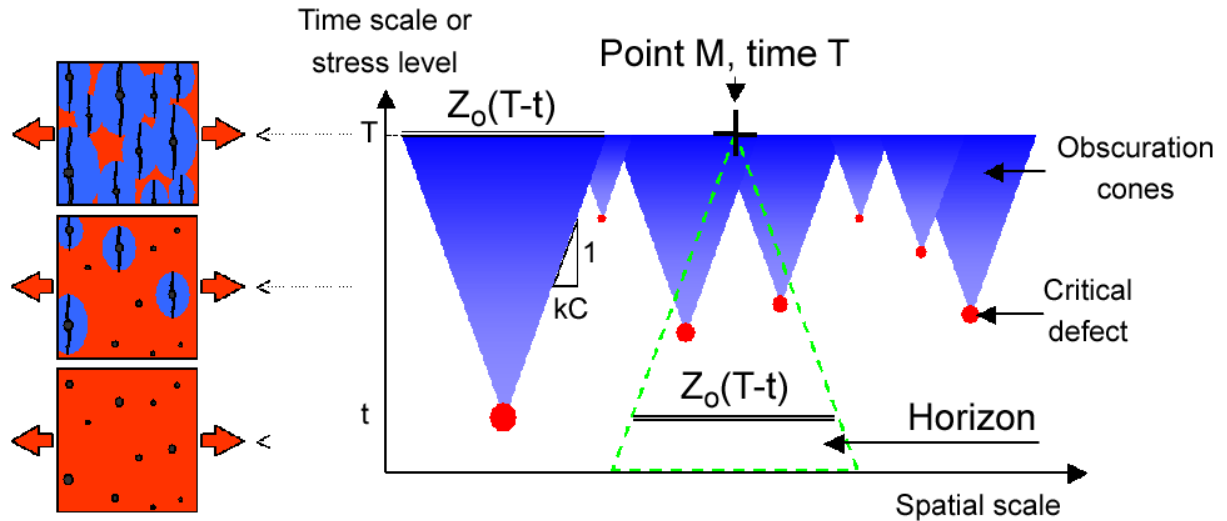
Figure 1. Obscuration phenomenon and horizon of a point (*M,T*) *(Forquin and Hild, 2010)*.

According to the concept of "local weakest link hypothesis" introduced in (Forquin and Hild, 2010) the probability of non-obscuration $P_{no}$ is equal to the product of the elementary probabilities of no new crack inception $P^i_{\notin}$ in each elementary space–time zones of $\Omega$ belonging to the horizon of the point $M$ at time $T$:

$$P_{no}(M,T) = \prod_{[horizon\ of\ (M,T)\in\Omega]} P^i_{\notin} \tag{1}$$

where $P^i_{\notin}$ is expressed as function of the density of critical defects $\lambda_t\ (x, t)$. If ones considers that $\lambda_t$ is a continuous function between $t$ and $t+dt$ $P^i_{\notin}$ reads:

$$P^i_{\notin}(\underline{x},t) = \exp\left(-\frac{\partial\lambda_t(\underline{x},t)}{\partial t}\,dZdt\right). \tag{2}$$

Otherwise if the density $\lambda_t\ (x, t)$ is discontinuous between $t_i$ and $t_i+dt$, expressing $\lambda_t(x, t_i+dt) - \lambda_t(x, t_i) = [\lambda_t]_{x,ti}$, the elementary probability of no-inception of new crack in the space-time area $dZ\ x\ dt$ located at $(x, t_i)$ is expressed as:

$$P^i_{\notin}(\underline{x},t_i) = \exp\left(-[\lambda_t]_{(\underline{x},t_i)}\,dZ\right). \tag{3}$$

Finally, by combining equations (1), (2) and (3) the non-obscuration probability at (*M, T*) takes the following expression:

$$P_{no}(M,T) = \exp\left(-\iint_{(\underline{x},t)\in[horizon\ of\ (M,T)\in\Omega]} \frac{\partial\lambda_t(\underline{x},t)}{\partial t}\,dZdt - \sum_i \int_{(\underline{x},t_i)\in[horizon\ of\ (M,T)\in\Omega]} [\lambda_t]_{(\underline{x},t_i)}\,dZ\right) \tag{4}$$

If one assume a zero density of cracks at time $T = 0$ the crack density can be obtained by integrating its derivate or summing its increments:

$$\lambda_{cracks}(M,T) = \int_0^T\left[\frac{\partial\lambda_{cracks}}{\partial t}(M,t)\right]dt + \sum_i[\lambda_{cracks}]_{M,t_i} \tag{5}$$

Given that new cracks are initiated only in the not-obscured part of the domain the increment of new cracks can be assumed to be proportional to the increment of critical defects weighted by the fraction

of non-obscured zones. Considering a fraction of non-obscured zones being equivalent to the probability of non-obscuration the increment and derivate of crack density reads:

$$\frac{\partial \lambda_{cracks}}{\partial t}(M,t) = P_{no}(M,t)\frac{\partial \lambda_t}{\partial t}(M,t), \; [\lambda_{cracks}]_{M,t_i} = P_{no}(M,t_i)[\lambda_t]_{M,t_i} \tag{6}$$

Finally, if one assumes as first approximation no interaction between cracks, the number of cracks generated in the domain at time *T* can be computed as a function of the crack density according to:

$$N_{cracks}(T) = \int_\Omega \lambda_{cracks}(M,T)dZ \tag{7}$$

In addition, in the case of a multiple fragmentation process, which corresponds to the non-interaction of the horizon of point (*M, T*) with the boundaries of the domain according to (Forquin et Hild, 2010), the probability of obscuration can be used as a damage variable *D*. Therefore, the macroscopic stress Σ can be calculated as function of the microscopic stress $\sigma$ such as:

$$\Sigma(T) = (1 - D(T))\sigma(T) \quad \text{with} \quad D(T) = 1 - P_{no}(T) \tag{8}$$

Therefore, the ultimate (maximum) macroscopic strength may be deduced:

$$\Sigma^u = \max_t \Sigma_{no}(t) = \Sigma_{no}(t^u) \quad \text{with} \quad \frac{d\Sigma_{no}}{dt}(t^u) = 0 \tag{9}$$

Finally, the knowledge of the density of critical defects appears to be essential to be able to predict the macroscopic strength and cracking density in brittle solids subjected to a high strain-rate tensile loading.

# 3    Predictions of DFH model considering a power-law function of $\lambda_t(\sigma)$

Two parameters need to be considered to be able to express the obscuration probability (Eq. 4): the density of critical defects and the shape of the horizon at point (*M, T*). In the present subsection the density of critical flaws is given in the form of a power law of the positive (tension) principal stress:

$$\lambda_t(\sigma_1) = \lambda_0\left(\frac{\langle\sigma_1\rangle}{S_0}\right)^m \tag{10}$$

In addition, considering that each zone of stress release (obscuration zone) is centered on the point of crack initiation and assuming that is grows in a self-similar way with a diameter proportional to the size of the crack the size of the zone of obscuration at a time T corresponding to a single crack created at time t can be expressed as:

$$Z_o\left[(T-t)\right] = S\left[kC(T-t)\right]^n \tag{11}$$

where *S* is a shape parameter of the obscuration volume (equal to 4 $\pi$ / 3 if ones assumes that obscuration volumes are similar to spheres in a 3D medium (*n* = 3), *S* = $\pi$ for a disc in a 2D medium (*n* = 2) or *S* = 2 in a 1D medium (*n* = 1)). When the horizon is strictly included inside the domain and if a uniform stress field is assumed, the obscuration probability corresponds to (Denoual and Hild, 2000):

$$P_o(M,T) = 1 - P_{no}(M,T) = 1 - \exp\left( -\int_0^T \frac{d\lambda_t}{dt}[\sigma(t)] \ Z_o(T-t)dt \right) \tag{12}$$

Moreover, assuming a constant stress rate ($\overset{\circ}{\sigma}$) an analytical closed-form solution of the obscuration probability (or equivalently the damage variable D) can be obtained as a function of three parameters, namely, $n$ the space dimension, $m$ the Weibull modulus, and $T/t_c$ the dimensionless time:

$$D(T) \equiv P_o = 1 - \exp\left( -\frac{m!n!}{(m+n)!}\left(\frac{T}{t_c}\right)^{m+n} \right) \tag{13}$$

The characteristic time $t_c$ is given by:

$$t_c = \underbrace{\left( \sigma_0 \lambda_o^{-\frac{1}{m}} \right)^{\frac{m}{m+n}}}_{Crack\ inception} \underbrace{\left( \dot{\sigma} \right)^{-\frac{m}{m+n}}}_{Loading\ rate} \underbrace{\left( S^{\frac{1}{n}}kC \right)^{-\frac{n}{m+n}}}_{Crack\ propagation} \tag{14}$$

For any value m > 3 and considering n = 3, the probability of obscuration is less than 5% at $T = t_c$ and it is greater than 95% at $T = 2t_c$. Therefore, the characteristic time represents the time during which most of the obscuration phenomenon occurs. In addition, a characteristic stress and a characteristic density may be defined in the following way:

$$\sigma_c = \overset{\circ}{\sigma}.t_c \quad \text{and} \quad \lambda_c = \lambda_t(\sigma_c) \tag{15, 16}$$

The corresponding closed-form solutions read:

$$\sigma_c = \underbrace{\left( \sigma_0 \lambda_o^{-\frac{1}{m}} \right)^{\frac{m}{m+n}}}_{Crack\ inception} \underbrace{\left( \dot{\sigma} \right)^{\frac{n}{m+n}}}_{Loading\ rate} \underbrace{\left( S^{\frac{1}{n}}kC \right)^{-\frac{n}{m+n}}}_{Crack\ propagation} \tag{17}$$

and

$$\lambda_c = \underbrace{\left( \sigma_0 \lambda_o^{-\frac{1}{m}} \right)^{-\frac{mn}{m+n}}}_{Crack\ inception} \underbrace{\left( \dot{\sigma} \right)^{\frac{mn}{m+n}}}_{Loading\ rate} \underbrace{\left( S^{\frac{1}{n}}kC \right)^{-\frac{mn}{m+n}}}_{Crack\ propagation} \tag{18}$$

By using the closed-form solution of the non-obscuration probability (Eq. 13) into the equations (5) and (6) the normalized crack density is obtained:

$$\frac{\lambda_{cracks}}{\lambda_c}(\sigma) = \frac{m}{m+n}\left[ \frac{(m+n)!}{m!n!} \right]^{\frac{m}{m+n}} \gamma\left( \frac{m}{m+n}, \frac{m!n!}{(m+n)!}\left(\frac{\sigma}{\sigma_c}\right)^{m+n} \right) \tag{19}$$

where $\gamma$ is the incomplete gamma function defined as:

$$\gamma(\alpha,T) = \int_0^T \exp(-t)t^{\alpha-1}dt \tag{20}$$

At the end of loading, the final crack density can be expressed as function of *m*, *n* and the characteristic density:

$$\frac{\lambda_{cracks}}{\lambda_c}(\sigma >> \sigma_c) = \left(\frac{(m+n)!}{m!n!}\right)^{\frac{m}{m+n}} \Gamma\left(1 + \frac{m}{m+n}\right) \tag{21}$$

In the same way, by using the closed-form solution of the non-obscuration probability (Eq. 13) into the equations (8) and (9) the ultimate macroscopic strength can be expressed as function of the characteristic stress:

$$\Sigma_{multiple}^u = \sigma_c \left(\frac{1}{e} \frac{(m+n-1)!}{m!n!}\right)^{\frac{1}{m+n}} \tag{22}$$

Equation (22) is used in the subsection 5.

# 4      Density of critical defects in three brittle materials

In the present works the microstructure of three different brittle materials (concrete, ceramic and polycrystalline ice) was examined prior testing. In order to identify the initial microstructure, a few samples of each material were scanned using two X-ray scanners available in 3SR and SIMaP laboratories. In both devices an X-ray source generates a beam which is collected by a panel detector. The sample is placed on a platform rotating around the vertical axis so the 3D image of the specimen is reconstructed from the acquired radiographs. By performing a thresholding, the image is binarized to identify the pores. Next, 3D image processing techniques are used to label the pores and to get their volumes. By approximating all the pores to spheres, the equivalent diameter distribution of each sample is obtained.

The first microstructure is an Ultra-High Performance Concretes (UHPC) that is characterised by a high compressive strength (above 140 MPa). The concrete formulation benefits from a reduced grain size ($\leq 0.5$ mm), a high level of particles packing and a small water to cement ratio (W/C $\leq 0.2$), so the amount of porosity is minimized. In order to identify the initial microstructure, a sample was scanned using the X-ray scanner in 3SR Laboratory with an achieved resolution corresponds to a pixel size of 70 $\mu$m.px$^{-1}$. The distribution of pore size is shown on the Fig. 2a. The second studied material is an artificial and equiaxed polycrystalline ice grown in laboratory (in the cold room of IGE). The final porosities and pore size distributions are controlled by the initial amount of air and the growth temperature. The pore size distribution obtained via X-ray tomography analysis allows assessing the sample reproducibility and homogeneity (Fig. 2b). The third microstructure is a dense SiC material in which a controlled porosity is introduced (Fig. 2c). The large pores are supposed to act as fusible flaws during a dynamic tensile loading preventing the crack initiation on smaller (and more numerous) pores, thus limiting the multi-fragmentation.
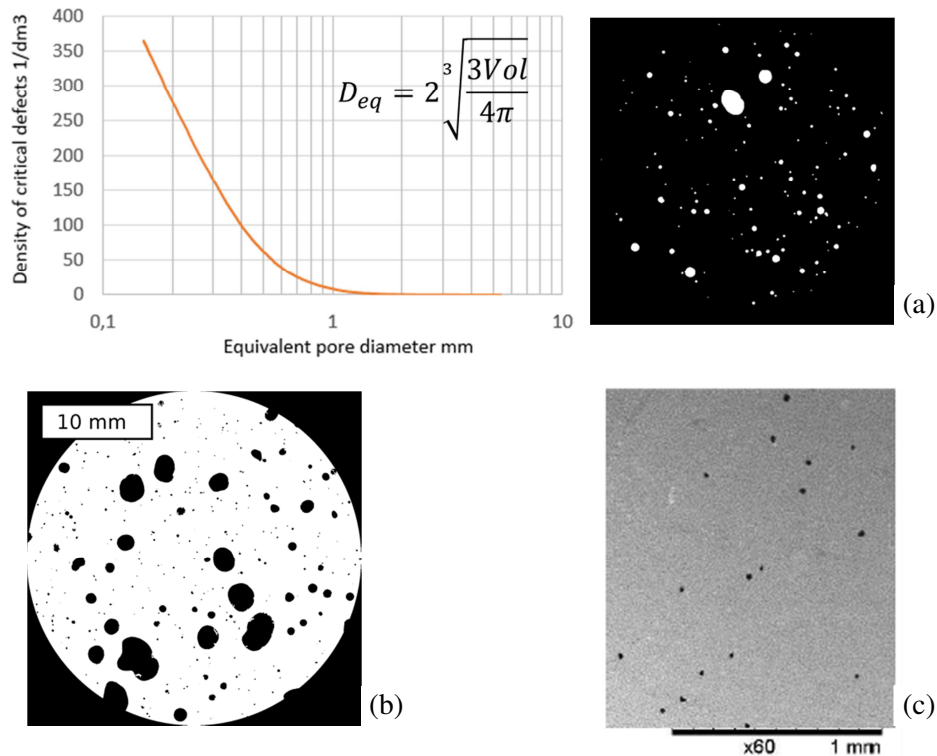
Figure 2. Three microstructures studied in the present work. (a) Distribution of pore size and binarized image by thresholding in an ultra-high performance concrete scanned with X-ray tomography system. (b) Slice view of an X-ray tomography scan from a high air content polycrystalline ice specimen. (c) SEM image of dense SiC material with added controlled porosity.

# 5     Predictions of the fragmentation properties of one brittle material based on tomographic analysis

In this last section the fragmentation properties of the UHPC are predicted based on the previous tomographic analysis. To do so, the previous cumulative distribution of pores provided in Fig. 2a (density of critical defects versus equivalent pore diameter) needs to be converted into a function of density of critical defects that is function of the applied microscopic stress. As previously introduced by several authors (Jayatilaka and Trustrum, 1977; Hild, 1992; Forquin et al, 2004) the linear fracture mechanics theory can be used to link the size of pores to their expected crack-inception stress. According to this theory the stress intensity factor $K_I$ related to a crack of size (2.$a$) is given by the following equation:

$$K_I = Y\sigma\sqrt{\pi a} \tag{23}$$

where $Y$ is a dimensionless correction factor, also often referred to as the geometric shape factor, that is related to the geometry of the crack. In the case of a straight crack of length (2.$a$) in an infinite plate having a uniform stress field and assuming this crack perpendicular to the loading direction this correction factor is ($Y = 1$). In the case of a penny-shaped crack of radius ($a$) in an infinite domain under uniaxial tension $\sigma$ the geometric shape factor is ($Y = 2/\pi$). Next, considering the critical stress intensity factor $K_{IC}$ of the tested material the macroscopic stress to trigger an unstable crack is given by:

$$\sigma_{trigger} = \frac{K_{IC}}{Y\sqrt{\pi a}} \qquad (24)$$

In the case of UHPC defect' population (Fig. 2a), the shape of flaws is complex and difficult to capture and a dimensionless parameter $Y$ different from 1 needs to be considered. This parameter was adjusted based on the results of three-point bending tests (not presented in the present paper). The best fit of data from bending tests was obtained with ($Y = 0.91$). Now, based on data from tomography analysis the density of critical defects can be plotted as function of their expected critical stress (Fig. 3a) and a polynomial function can be easily fitted such as:

$$\lambda_t(\sigma) = \exp(\sum_{i=0}^{n} a_i(\sigma)^i) \qquad (25)$$

Finally, considering a linear increate of microscopic stress as function of time ($\sigma(t) = \sigma°.t$) the obscuration probability was calculated by double integration of the following equation derived from Equation (12):

$$\frac{d^{n-1}}{dt^{n-1}}\left(\frac{1}{1-P_o}\frac{dP_o}{dt}\right) = n!\,S(kC)^n\lambda_t(\sigma) \qquad (26)$$

with the following parameters ($n = 3$, $S = 3.74$, $kC = 1856$ m/s). By introducing the density of critical defects of Eq. (25) into the Eq. (26) the obscuration probability evolution is obtained so the cracking density and the macroscopic stress provided by Equations (6) and (9) are deduced. Lastly, the final cracking density and the ultimate macroscopic strength can be depicted as function of the strain-rate. The predicted the macroscopic strength of the UHPC is plotted as function of the strain-rate considering both the Weibull density of critical defects (power law function) and the identified function of Fig. 3a. Whereas a good match is obtained at low strain-rate, at high strain-rate, a higher level of strength is predicted with the population of defects identified from the tomography analysis compared to the Weibull population of defects. The main reason is that, at the highest strain-rates, numerous small defects are activated that are not captured by the Weibull power-law function. Finally this approach demonstrates the interest to consider a defect' population identified from tomography rather than from bending tests performed by considering a single sample size.
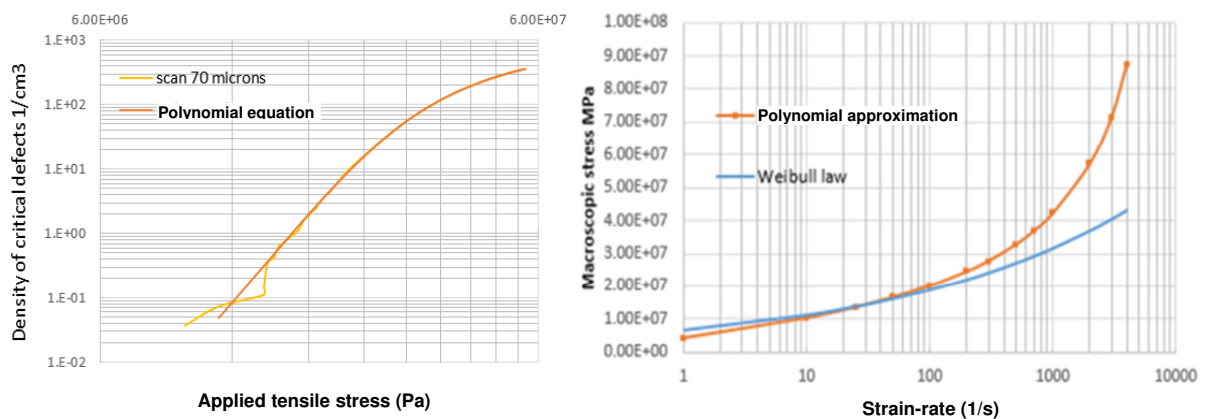


Figure 3. (a) Identification of the density of critical defects as function of the applied stress. (b) Predictions of the macroscopic strength as function of the strain-rate considering (i) a density of critical defects as a power law function of the applied stress (Weibull law) and (ii) the identified function of Figure 3a.

# 6     Conclusion

In the present paper a new methodology is proposed to model the multiple fragmentation process in brittle solids based on data provided by micro-tomography analysis. Samples of three different kinds of brittle materials, an ultra-high performance concrete, a polycrystalline ice and a SiC ceramic in which a controlled porosity made of large pores was introduced, have been analysed through an X-ray tomography analysis. A processing of data allows the pore size distribution to be deduced. By leaning on the linear fracture mechanics theory the density of critical defects is expressed as function of the applied stress. Finally, general equations of Denoual-Forquin-Hild obscuration model are applied with the deduced density of critical defects. Predictions can be made in terms of final cracking density and ultimate macroscopic strength as function of the applied strain-rate. This methodology applied to the data of the UHPC reveals that the obtained predictions at the highest strain-rates may differ from the results provided by the classical Weibull approach. Finally, the tomography analysis constitutes a promising approach to improve the predictions of dynamic fragmentation process over a large range of strain-rates.

# References

Denoual C., Hild F., 2000. A damage model for the dynamic fragmentation of brittle solids, Computer Methods in Applied Mechanics and Engineering, 183, 247-258

Forquin P., Hild F., 2010. A probabilistic damage model of the dynamic fragmentation process in brittle materials, Advances in Applied Mechanics, 44, 1-72

Forquin, P., Charles, Y., Rota, L., Hild, F., 2004. A method to determine the macroscopic toughness scatter of brittle materials, Int. J. Fracture, 125 (1), 171-187

Hild F., 1992. De la rupture des materiaux à comportement fragile. Sciences de l'ingénieur [physics]. Université Pierre et Marie Curie - Paris VI. Français. tel-00460367

Jayatilaca A. D. S., Trustmm K., 1977. Statistical approach to brittle fracture, J. Mat. Sci., 12 , 1426-1430